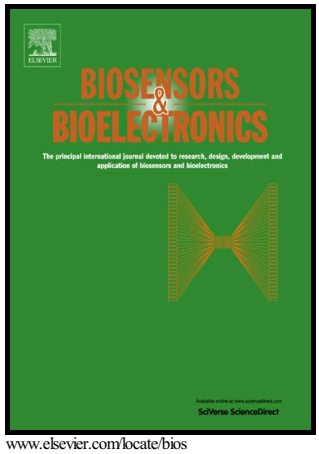

www.elsevier.com/locate/bios

Detection of Regional DNA Methylation Using DNA-Graphene Affinity Interactions

Hakimul Haque, Vinod Gopalan, Sharda Yadav, Md Nazmul Islam, Ehsan Eftekhari, Qin Li, Laura G. Carrascosa, Nam-Trung Nguyen, Alfred K. Lam, Muhammad J.A. Shiddiky

PII: S0956-5663(16)30887-9
DOI: http://dx.doi.org/10.1016/j.bios.2016.09.016
Reference: BIOS9128

To appear in: *Biosensors and Bioelectronic*

Received date: 3 June 2016
Revised date: 29 August 2016
Accepted date: 4 September 2016

Cite this article as: Hakimul Haque, Vinod Gopalan, Sharda Yadav, Md Nazmul Islam, Ehsan Eftekhari, Qin Li, Laura G. Carrascosa, Nam-Trung Nguyen Alfred K. Lam and Muhammad J.A. Shiddiky, Detection of Regional DNA Methylation Using DNA-Graphene Affinity Interactions, *Biosensors and Bioelectronic,* http://dx.doi.org/10.1016/j.bios.2016.09.016

Detection of Regional DNA Methylation Using DNA-Graphene Affinity Interactions

Md. Hakimul Haque[abc], Vinod Gopalan[a]*, Sharda Yadav[b,c], Md Nazmul Islam[b,c], Ehsan Eftekhari[c,d], Qin Li[c,d], Laura G. Carrascosa[e], Nam-Trung Nguyen[c], Alfred K. Lam[a]*, Muhammad J. A. Shiddiky[b,c]*

[a]Cancer Molecular Pathology Laboratory in School of Medicine, Menzies Health Institute Queensland, Griffith University, Gold Coast Campus, Australia

[b]School of Natural Sciences, Griffith University, Nathan Campus, QLD 4111, Australia

[c]Queensland Micro and Nanotechnology Centre, Griffith University, Nathan Campus, QLD 4111, Australia

[d]School of Engineering, Griffith University, Nathan, QLD 4111, Australia

[e]The University of Queensland, Brisbane, QLD 4072, Australia

v.gopalan@griffith.edu.au(VG)

a.lam@griffith.edu.au (AKL)

m.shiddiky@griffith.edu.au(MJAS)

*Corresponding author.

Abstract

We report a new method for the detection of regional DNA methylation using base-dependent affinity interaction (i.e., adsoption) of DNA with graphene. Due to the strongest adsorption affinity of guanine bases towards graphene, bisulfite-treated guanine-enriched methylated DNA leads to a larger amount of the adsorbed DNA on the graphene-modified

electrodes in comparison to the adenine-enriched unmethylated DNA. The level of the methylation is quantified by monitoring the differential pulse voltammetric current as a function of the adsorbed DNA. The assay is sensitive to distinguish methylated and unmethylated DNA sequences at single CpG resolution by differentiating changes in DNA methylation as low as 5%. Furthermore, this method has been used to detect methylation levels in a collection of DNA samples taken from oesophageal cancer tissues.

Keywords

DNA methylation, Regional methylation, Electrochemical detection, Graphene-DNA base interaction, Disposable screen-printed electrode

1. Introduction

DNA methylation is a cell-type specific epigenetic marker, essential for controlling gene expression via transcriptional regulation, silencing of repetitive DNA and genomic imprinting (Jones and Takai, 2001; Wu and Zhang, 2010). Current advances in DNA methylation research have suggested that different types of cancers appear to have distinct DNA methylation levels at selected regions (*i.e.*, regional methylation), which are responsible for their various responses to treatment (Taleat et al., 2015; Zhang et al., 2015). For example, regional methylation plays a fundamental role in the initiation and progression of oesophageal squamous cell carcinoma (ESCC) by inactivating transcription and loss of gene function (Chang et al., 2002; Delpu et al., 2013; Wong et al., 2006; Wong et al., 2003). Also,

DNA methylation based biomarker has proven to be used alone or in combination with other diagnostic methods in cancer (Delpu et al., 2013). Thus, detection of methylation in targeted cancer specific genes could have diagnostic and prognostic implications in human cancers.

Over the past several decades, a number of conventional molecular biology approaches, including-bisulfite sequencing, MS-PCR, mass spectrometry and fluorescence based methods have been extensively used to measure the level of DNA methylation in cancers (Herman et al., 1996; Cao and Zhang, 2012; Zhang et al., 2011; Plongthongkum et al., 2014; Taleat et al., 2015; Zhang et al., 2015). These approaches employed sequencing, mass spectrometric or fluorescence readouts to differentiate between methylated and unmethylated sequences. They are relatively robust but are limited by the costly instruments, DNA fragmentation, chimeric product generation, fluorescent labels and long analysis time. Furthermore, these methods are limited by the background fluorescence interference as well as to high labour and bioinformatics costs.

In the recent years, much attention has been focused on developing inexpensive and faster detection strategies based on colorimetry, electrochemistry, Raman scattering readouts (Carrascosa et al., 2014; Kato et al., 2011; Kato et al., 2008; Koo et al., 2014b; Kurita et al., 2012; Taleat et al., 2015; Wang et al., 2016; Wee et al., 2015a; Wee et al., 2015b; Zhang et al., 2015). While all these methods have many advantages, their sensor fabrication procedure and data deconvolution methods are rather complicated due to the involvement of complex surface functionalisation steps or coupling chemistry (Carrascosa et al., 2014; Kato et al., 2011; Kato et al., 2008; Koo et al., 2014b; Kurita et al., 2012; Taleat et al., 2015; Wang et al., 2016; Wee et al., 2015a; Wee et al., 2015b; Zhang et al., 2015). Therefore, a simple and inexpensive method that could simplify the detection method by avoiding the complicated chemistry underlying each step of the sensor fabrication represents an appealing alternative to alleviate some of these issues.

More recently, we have reported a simple method for quantifying DNA methylation using different adsorption affinity of DNA bases onto an unmodified gold substrate (Koo et al., 2014a; Sina et al., 2014). Similar to gold substrate, graphene (Varghese et al., 2009) and graphene oxide (Wu et al., 2011) have been reported as promising substrates for adsorbing nucleobases and nucleosides. Over the past few years, several fundamental studies have been carried out to explore the nature of the direct interaction (*i.e.*, adsorption) of nucleobases and nucleosides onto the graphene and graphene oxide surface (Gowtham et al., 2007; Varghese et al., 2009; Wu et al., 2011). These studies have suggested that the physisorption between individual nucleobases and the graphene (*i.e.*, adsorption on graphene) is controlled by the polarisabilities of the individual nucleobases. Among all nucleobases, guanine and adenine with their five- and six-membered rings possess the largest polarisabilities, whereas other bases with only six-membered rings exhibit lower polarisabilities. Additionally, guanines with its double-bonded oxygen atom possess a larger polarisability than adenine. Since the van der Wall (vdW) energy is directly proportional to the interacting nucleobases, Scheicher (Gowtham et al., 2007) and Rao (Varghese et al., 2009) have proposed that vdW interaction is indeed the main driving force for the adsorption of nucleobases onto the graphene and follows the adsorption trend as guanine (G)> adenine (A)> thymine (T)> cytosine (C). Because this interaction is base (*i.e.*, sequence) dependent and bisulfite conversion generates two DNA sequences with different base compositions, bisulfite-converted two DNA sequences should give different adsorption patterns on graphene surface. To date, there is no other method that uses the graphene-DNA affinity interaction to quantify DNA methylation.

Herein, we report a simple and inexpensive method for detecting regional DNA methylation using direct adsorption of bisulfite-treated and PCR amplified DNA sequences onto graphene-modified screen-printed carbon electrode (g-SPCE). In this approach, following the bisulfite conversion and asymmetric PCR amplifications steps, the amplified

products was directly adsorbed on g-SPCE. The relative adsorption of the amplified products was then detected *via* differential pulse voltammetry (DPV) in the presence of the $[Fe(CN)_6]^{3-/4-}$ redox system. We first optimized the adsorption parameters (*i.e.*, adsorption time, pH of the solution, etc) to achieve optimal analytical performance of the method. Then, we applied this method to detect *FAM134B* promoter gene methylation in a panel of ESCC cell lines and patient samples derived from oesophageal squamous cell carcinoma. Finally, we established a correlation between promoter hypermethylation and *FAM134B* gene expression levels.

2. Experimental

2.1 Materials

All reagents were of analytical grade and purchased from Sigma Aldrich (St Louis, MO, USA). UltraPureTM DNase/RNase-free distilled water (Invitrogen, Carlsbad, CA, USA) was used throughout the experiments. Jurkat 100% methylated genomic DNA was purchased from New England Biolabs (Ipswich, MA, USA). Two oesophageal squamous cell carcinoma (ESCC) cell lines, HKESC-1 and HKESC-4, were kindly gifted from Department of Pathology, University of Hong Kong. Another ESCC cell line- KYSE-510 was purchased from Leibniz Institute DSMZ (German collection of microorganisms and cell cultures). All these cell lines were grown in minimum essential medium alpha (MEMα growth medium, Gibco (ThermFisher scientific, Waltham, MA, USA) medium with non-essential amino acids supplemented with 10% fetal bovine serum (FBS, Gibco), 100 µg/mL penicillin (Gibco) and 100 unit/mL streptomycin (Gibco) in a humidified cell culture incubator containing 5% CO_2 at 37°C. Graphene-modified screen-printed carbon electrodes (g-SPCE, 110GPH) were acquired from Dropsens (Spain).

2.2 Clinical samples

Surgically resected fresh tissue samples (cancer and matched non-cancer) from eight ESCC patients were used for this study. Histopathological confirmation of carcinoma was made prior to DNA isolation. All ESCC patients selected in this study were free from radio/chemotherapy and were matched with gender (all male) and clinical staging (stage III & IV). Mean age group of the patients were 65± 14, ranging from 45-74 years. Ethical approval has been obtained for the use of these samples (GU Ref No: MED/19/08/HREC). The selected samples were sectioned using a cryostat (Leica CM 1850 UV, Wetzlar, Germany) and stained by haematoxylin and eosin.

2.3 *Genomic DNA extraction*

HKESC-1, HKESC-4 and KYSE-510 ESCC cell lines were grown in minimum essential medium alpha (MEMα growth medium, Gibco (ThermFisher scientific, Waltham, MA, USA) medium with non-essential amino acids supplemented with 10% fetal bovine serum (FBS, Gibco), 100 µg/mL penicillin (Gibco) and 100 unit/mL streptomycin (Gibco) in a humidified cell culture incubator containing 5% CO_2 at 37°C. Genomic DNA was extracted and purified from 10^5 cell plates of the aforesaid cell lines and clinical samples using DNeasy blood and tissue kit (Qiagen Pty. Ltd., Venlo, Netherlands) following manufacturer's instructions. Briefly, after harvesting, appropriate number of cells was suspended in phosphate buffer solutions. A digestion step was executed to remove the protein and RNA in the solution via proteinase and RNase enzymes, respectively. Then, cell samples were suspended in lysis buffer to disrupt and release the nucleic acids and proteins into the solution. The digested proteins and RNA were removed by centrifuging the solution in a spin column. The purified DNA was eluted from the column in 100 µL of elution buffer and stored at -20°C. The whole

genomic amplified (WGA) DNA samples was prepared through amplifying about 50 ng genomic DNA using REPLI-g whole genome amplification kit (Qiagen Pty. Ltd., Venlo, Netherlands) according to manufacturer's instructions. DNA quantification was achieved via Nanodrop Spectrophotometer (BioLab, Ipswich, MA, USA) and purity was measured using 260/280 ratio. Concentration of DNA was noted in ng/µL and then stored at -20˚C until use.

2.4 *Bisulphite treatment*

MethylEasy™ Xceed kit (Human Genetic Signatures Pty. Ltd., NSW, Australia) was used to perform bisulphite conversion as per the manufacturer instruction. Briefly, 500 ng of DNA were incubated with 150 mM NaOH solution at 37 °C for 15 minutes followed by treatment with sodium bisulfite at 80 °C for 45 minutes. Then bisulfite-treated DNA solution was purified using the protocol from MethylEasy™ Xceed kit. DNA quantification and purity was checked *via* Nanodrop Spectrophotometer (BioLab, Ipswich, MA, USA). Concentration of bisulphite treated DNA was noted in ng/µL and then stored at -20˚C until use.

2.5 Normalization of DNA copy number

In order to normalize the DNA copy number from each DNA source, the relative amount of *FAM134B (JK1)* genes in bisulphite treated cell and WGA DNA samples were determined by real-time amplification of the house keeping *HBD* gene using the Rotor-Gene Q detection system (Qiagen, Hilden, Germany) and performing comparative analysis of Ct (*i.e.* the fractional PCR cycle number at which the reporter fluorescence is greater than the threshold). qRT-PCR was performed in a total volume of 10 µL reaction mixture comprising 5 µL of 2XSensiMix SYBR No-ROX master mix (Bioline, London, UK), 1 µL of each 250 nM primer, 1 µL of equal concentrated target cell and WGA DNA samples with 2 µL of

nuclease-free water. Thermal cycling programs encompassed initial denaturation and activate the hot start DNA polymerase in one cycle of 7 minutes at 95 °C followed by 40 cycles of 10 seconds at 95°C (denaturation), 30 seconds at 60°C (annealing) and 20 seconds at 72°C (extension).

2.6 *Asymmetric PCR*

Asymmetric PCR of the bisulphite treated DNA was carried out using AmpliTaq Gold 360 master mix (ThermFisher scientific, Waltham, MA USA) to generate ss-DNA amplicons. Asymmetric PCR was performed by suing 60 µL reaction mixture comprising 30 µL of AmpliTaq Gold 360 master mix, 1 µL of 125 nM forward primer and 375 nm reverse primer (see Table S1), 1 µL of 50 ng bisulphite treated DNA and 28 µL of nuclease-free water. PCR cycling programs was performed under the following conditions: 95°C for 10 minutes followed by 49 cycles of 30 seconds at 95°C (denaturation), 30 seconds at 61°C (annealing) and 20 seconds at 72°C (extension).

2.7 Methylation specific-high resolution melting (MS-HRM) curve analysis

MS-HRM was performed according to the modified versions of the previously published procedure (Wojdacz and Dobrovic, 2007). Briefly, HRM curve analysis was carried out on the Rotor-Gene Q detection system (Qiagen) using the Rotor-Gene ScreenClust Software. PCR was performed in a 10 µL total volume containing 5 µL of 2Xsensimix HRM master mix, 1 µL of 20 ng/µL bisulfite modified genomic DNA, 2 µL RNase free water and 1 µL of each primer. The thermal profile comprised 15 min at 95°C, followed by 50 cycles of 30 seconds at 95°C, 30 seconds at 61°C and 20 second at 72°C. High resolution melting analyses were carried out at temperature ramping from 70-95°C. The normalization of

melting curve were performed following the previous procedure (Wojdacz and Dobrovic, 2007).

2.8 Electrochemical measurements of DNA methylation

All electrochemical measurements were performed on a CH1040C potentiostat (CH Instruments, Bee Cave, TX, USA) with the three-electrode system printed on a ceramic substrate (length 33 x width 10 x height 0.5) mm. In the three-electrode system, working (diameter = 4mm), counter and reference electrodes were graphene/carbon, carbon, and silver-modified electrodes. Differential pulse voltammetry experiments were conducted in 10 mM phosphate buffered saline (PBS) solution containing 2.5mM [$K_3Fe(CN)_6$] and 2.5mM [$K_4Fe(CN)_6$] electrolyte solution. DPV signals were obtained with a potential step of 5 mV, pulse amplitude of 50 mV, pulse width of 50 ms, and pulse period of 100 ms. For synthetic DNA samples, 8 µL (diluted in SSC5X buffer to get 100 nM of DNA) sample was adsorbed on g-SPCE surface. For cell lines and clinical samples analysis, 10 times-diluted amplified products (i.e., 20 µL of amplified DNA spiked in 200 µL of SSC5X buffer) were used for adsorption experiments. The electrodes were then washed three times with PBS prior to perform DPV measurements. The relative DPV current changes (*i.e.*, $\%I_{\text{Relative}}$, percent difference of the DPV signals generated for DNA sample (I_{Sample}) with respect to the baseline current (I_{Baseline})) due to the adsorption of DNA samples were then measured by using equation 1. The difference in relative DPV signals between unmethylated and methylated DNA was calculated by using equation 2.

$$\%I_{Relative} = \frac{\%I_{Baseline} - \%I_{Sample}}{\%I_{Baseline}} \times 100 \quad \ldots\ldots (1)$$

$$\Delta I_{\text{Relative}} = \%I_{\text{Relative, M}} - \%I_{\text{Relative, UM}} \quad \ldots\ldots (2)$$

where $\%I_{\text{Relative, M}}$ and $\%I_{\text{Relative, UM}}$ are the relative DPV signals for the methylated, and unmethylated samples, respectively.

2.9 Fourier Transform Infrared Spectroscopy and UV-Vis Experiments

Fourier Transform Infrared Spectroscopy (FTIR) spectra were collected on a Perkin-Elmer Spectrum 100 with a resolution of 4 cm^{-1} in absorption mode. A baseline correction was applied after the measurement. The measurements were performed for a bare graphene-modified and DNA/graphene-modified working electrode. UV-vis absorption spectra were measured on Agilent 8453 UV-Vis spectrometer. The UV-vis measurements were done in aqueous solution.

3 Results and discussion

3.1 Principle

Fig. 1 illustrates the principle of the method. Briefly, ds-DNAs were first extracted from the cancer cell lines. A bisulfite conversion step was then performed to convert unmethylated cytosines in ds-DNA (double stranded DNA) into uracils while methylated cytosines remain unchanged. In a subsequent asymmetric PCR amplification step, all ds-DNA were converted to ss-DNA (single stranded DNA) amplicons. In this step, cytosines in the complementary strand will be copied to guanines and uracils to adenines resulting in methylated sample into guanine-enriched and unmethylated into adenine-enriched ss-DNA. These samples were then directly adsorbed on the g-SPCE surface. The DNA-attached g-SPCE surfaces were characterised by FTIR analysis. The interaction between graphene and DNA sequences has

also been tested in solution phase *via* UV-Vis spectrometry (for details see text and Fig S1 in Supplementary Material). The adsorbed ss-DNA amplicons were detected by differential pulse voltammetry (DPV) in the presence of a small redox active $[Fe(CN)_6]^{3-/4-}$ group. Previously, we (Koo et al., 2014a; Sina et al., 2014) and Zhang *et al.* (Zhang et al., 2007) have shown that unlike conventional redox system (*e.g.*, $[Ru(NH_3)_6]^{3+}/[Fe(CN)_6]^{3-}$) (Das et al., 2012), the $[Fe(CN)_6]^{3-/4-}$ alone is sufficient for quantifying surface-bound sequences reliably. As outlined by Zhang *et al.* (Zhang et al. 2007), the process follows an electron transfer kinetics-based mechanism, where density of the adsorbed DNA sequences at the electrode surface should be sufficiently low (*i.e.*, partial blocking). Under this condition, the columbic repulsion between the surface-bound ss-DNA and $[Fe(CN)_6]^{3-}$ is not strong enough to fully repel $[Fe(CN)_6]^{3-}$molecules from accessing the surface. Therefore, it generates a significant DPV signal which is lower than that of the un-modified electrode (*i.e.*, before ss-DNA adsorption) (Koo et al., 2014a; Sina et al., 2014). In the current method, since the adsorption strength of DNA bases towards graphene vary as G>A>T>C, the guanine-enriched methylated DNA leads to a larger level of adsorbed DNA on the electrodes in comparison to the adenine-enriched unmethylated DNA. Hence, as schematically shown in Fig.1, methylated DNA results in a smaller DPV current (*i.e.*, larger relative current change, $\%I_{Relative}$).

We have first explored the oncogenic properties and altered expression of *FAM134B (JK1)* gene in oesophageal squamous cell carcinoma (Tang et al., 2007). Also, *FAM134B* has been reported to have roles in pathogenesis as well as prediction of prognosis of other gastrointestinal cancer, namely colorectal cancer (Kasem et al., 2014). Most current approaches detect DNA methylation in oesophageal cancers via methylation specific PCR amplification process (Kuroki et al., 2003; Long et al., 2007). In this proof-of-concept study,

we have used graphene-DNA affinity interaction for detecting gene-specific DNA methylation in *FAM134B*. Firstly, the *FAM134B* promoter region containing 11 CpG sites located within a length of 60 bases was chosen as a target DNA. In order to further validate our approach, we have designed synthetic samples containing 0, 1, 5 and 11 CpG sites within the promoter region of *FAM134B* gene which mimic the bisulfite treated and asymmetric PCR processed methylated and unmethylated DNA regions (See Table S1, Supplementary Material).

One of the key considerations of the current method is that there is only a finite amount of electrode area and we should have the right amount of adsorbed DNA on the electrode surface so that the extent of methylation makes discernible signal difference. Therefore, we first optimised adsorption time and pH of the solution to achieve optimal amount of adsorbed DNA on the electrode surface so that the affinities of the DNA with different amounts of methylation can be discerned. Relative current differences ($\Delta I_{\text{Relative,}}$ see Experimental) between the 100 nM methylated (11 CpG) and unmethylated (0 CpG) DNA samples were measured. As seen in Fig. S2, an adsorption time of only 1 min is sufficient to generate a significant $\Delta I_{\text{Relative}}$ value. The maximum $\Delta I_{\text{Relative}}$ was found at 2 min, which was rapidly decreased with increasing adsorption time. Long adsorption time (>10 min) would lead to large amount of adsorbed DNA (*i.e.*, complete block of the surface) on electrode surface. This results in a similar level of columbic repulsion between the surface-bound DNA and $[Fe(CN)_6]^{3-}$ for both the methylated and unmethylated cases, providing two DPV signals with almost identical magnitudes leading to a small $\Delta I_{\text{Relative}}$ changes.

We then evaluated the pH-dependent $\Delta I_{\text{Relative}}$ changes by varying the pH of the solution from 3.0 to 9.5 (Fig. S3). Clearly, both methylated and unmethylated DNA samples could be distinguished at all the pH examined. The optimal $\Delta I_{\text{Relative}}$ value was found at pH

7.4. This can be explained by the fact that negative charge of the phosphate backbone of DNA at this pH is optimal to hinder the graphene-DNA interaction for both methylated and unmethylated samples while still allowing the methylated DNA with higher guanine contents to be interacted strongly. At the lower pH, the N3 position of the cytosines in methylated and unmethylated sequences can be protonated (p*K*a = 4.2) (Wu et al., 2011). This may contribute to reduce the Van-der Wall interaction (*i.e.,* electrostatic repulsion) between targets sequences and graphene surface, and thus result in a lower adsorption, leading to higher DPV currents (*i.e.,* lower $\Delta I_{\text{Relative}}$ changes). At the higher pH, the electrostatic interaction (adsorption) between graphene and DNA sequences is very strong, which significantly contribute to facilitate their adsorption on graphene-modified surfaces (*i.e*., both targets reach to the saturation level within a very short time giving a reduced $\Delta I_{\text{Relative}}$ value).

The main advantage of gold standard sequencing-bisulfite based method is that they can detect DNA methylation with single-base resolution. To evaluate the feasibility of our assay for detecting a minimum number of CpG methylation, four synthetic DNA samples containing 0, 1, 5 and 11 CpG sites were tested (as outlined above and in Table S1, Supplementary Material). Fig. 2 shows that the decrease of the relative current changes is a function of the number of CpG cites. This is due to the increase of the guanine contents with increasing methylated CpG sites in the target sequence. The level of relative adsorption pattern of methylated CpG sites agreeably implies the high specificity of our assay for effective detection of DNA methylation at a single CpG level of resolution.

Since tissue samples from patients with cancer usually contain a mixture of methylated and unmethylated DNA, accurate quantification of heterogeneous DNA methylation pattern is significant for detection and prediction of various clinicopathological parameters in cancers. It is therefore important to detect the degree of methylation in a high background of unmethylated DNA samples. To evaluate the assay performance for detecting

heterogeneous DNA methylation pattern, we analysed the dependence of the relative current changes on various degree of methylation. The samples were prepared by mixing synthetic standards of methylated and unmethylated DNA sequences to get 0%, 5%, 25%, 50%, 75%, 95% and 100% methylation, Fig. 3. The relative current changes (%$I_{Relative}$) increases with increasing levels of methylation, probably due to the increasing guanine contents in the target DNA sequences (*i.e.*, low DPV current and thus the higher %$I_{Relative}$). The linear regression equation was y (%$I_{Relative}$) = 2.3193x + 20.77(C) with a correlation coefficient (r^2) of 0.9921. A methylation change as low as 5% could be detected from 100 nM of DNA. These data was much better than our previous gold-DNA based approach (Koo et al. 2014a; Sina et al. 2014) and was of comparable to recent approaches (Carrascosa et al., 2014; Koo et al., 2014b; Wang et al., 2016; Wee et al., 2015a; Wee et al., 2015b), and clearly demonstrate that our approach is both specific and sensitive in detecting methylated DNA in the nanogram regime.

To test the applicability of our assay for detecting methylation level of *FAM134B* promoter gene, DNA samples derived from three ESSC cell lines were tested, Fig. 4A. A fully unmethylated whole genome amplified DNA was used as an internal standard. For avoiding any PCR bias, as outlined in our previously reported *methylsorb* assay (Koo et al., 2014a; Sina et al., 2014), we normalized the gene copy number prior to PCR amplification (see Experimental for details). As expected, for all the three cancer cell lines and WGA samples, significant relative current changes were observed indicating the presence of different degree of methylation. Importantly, two of the cell-derived samples (*i.e.*, KYSE-510 and HKESC-1) resulted in a large relative current changes when compared to that of the unmethylated WGA (*e.g.*, $\Delta I_{Relative}$ between KYSE-510 cell lines and unmethylated WGA was found to be ~14.6%), indicating DNA sequence derived from KYSE-510 and HKESC-1 cell lines could be hypermethylated at *FAM134B* promoter gene. These data clearly indicate

that the proposed assay may be a useful alternative for detecting *FAM134B* promoter gene methylation in cell-derived samples.

To further demonstrate the applicability of our method in analysing clinical samples, we extended our assay to analyse six tissue DNA samples derived from patients with primary oesophageal squamous cell carcinoma. Two oesophageal non-cancerous tissue DNA samples were also used as a control (see Experimental for details). Fig. 4B indicates that all samples showed different degree of methylation. The level of relative current changes with respect to that of the WGA obtained for two normal samples clearly show that these two samples are unmethylated. Also by comparing the level of relative current changes found in cell lines (Fig. 4A), we can estimate that four DNA samples derived from P3, P4, P5 and P6 cancer patients were highly methylated, while P1 and P2 samples were partially methylated (i.e., low methylation) at *FAM134B* promoter gene. We then validated our assay performance with well-known MS-HRM curve analysis. As can be seen in Fig S5, WGA and N1 samples have almost similar methylation level. Also the P6 sample has relatively higher methylation level compare to that of the P2 sample. These data are in-line with our adsorption based data.

Previously, it has been reported that gene silencing due to promoter hypermethylation play a fundamental role in pathogenesis of oesophageal squamous cell carcinoma (Wong et al. 2006). To evaluate whether the promoter hypermethylation of the *FAM134B* gene is linked with oesophageal cancer development, the *FAM134B* mRNA expression in all studied samples were examined *via* qRT-PCR (see Fig. S4 and experimental details in Supplementary Material). While our assay have showed higher level of methylation (*i.e.*, aberrant promoter hypermethylation) of the *FAM134B* gene in four primary cancer patients (P3, P4, P5 and P6 in Fig 4B), the mRNA expression study revealed under-expression in three of these DNA samples (P4, P5 and P6, Fig S4 in Supplementary Material). Furthermore, mRNA over-expression was found in three patient samples (P1, P2, P3),

indicating that the associated CpG region could be unmethylated or partially methylated. In our assay, we have noted that the levels of methylation for P1 and P2 samples are slightly higher than those of WGA (see Fig. 4A) and normal samples (N1 and N2 in Fig. 4B), indicating that these two samples (P1 and P2) could be partially methylated, and is in good agreement with RNA-expression data. In contrast, P3 sample showed significantly higher methylation levels than normal and WGA samples. This outcome suggests that this region could be hypermethylated, in disagreement with our mRNA expression data. The electrochemical data presented here clearly suggests that there is a relationship between promoter methylation level and mRNA expression of *FAM134B* gene in oesophageal squamous cell carcinoma, and support the accuracy of our assay. Although an in-depth study is needed to fully evaluate and validate clinical utility of the method, the analytical performance of the assay in its current form suggests the high feasibility of our assay in clinical sample analysis.

4 Conclusion

We have developed a simple and new method for the quantification of gene-associated DNA methylation using affinity interaction between DNA bases and graphene. The method is based on the different adsorption affinity of DNA nucleotides towards graphene-modified electrodes. The detection was achieved by the direct adsorption of two sequentially different DNA samples (bisulfite-treated and PCR amplified sequences representing methylated and unmethylated DNA) onto a graphene-modified electrode, which avoids multiple modifications and functionalisation steps involved in conventional assays. Furthermore, it avoids the need for sequencing analysis. Most importantly, we have tested the feasibility of our assay to detect methylation target of *FAM134B* promoter gene in a panel of ESCC cell lines and clinical samples from ESCC patients. We anticipated that our assay might be able to detect global hypomethylation since the methylated and unmethylated DNA-base changes of

bisulfite treated genomes entails a large number of CpG sites, which might generate a marked adsorption difference between fully methylated and partially methylated samples. In addition, our assay could be viably useful in clinical diagnostics because of its potential for accurate detection of epigenetic biomarker.

Acknowledgement

This work was supported by the NHMRC CDF (APP1088966 to M.J.A.S.), Griffith University New Researcher Grant Scheme and higher degree research scholarships (GUIPRS and GUPRS scholarships to M.H.H. and M.N.I.) from the Griffith University.

Appendix A. Supplementary Material

Supplementary data associated with this article can be found in the online version at http://

References

Cao, A., Zhang, C.Y. 2012. Anal Chem.84, 6199-6205.

Carrascosa, L.G., Sina, A.A., Palanisamy, R., Sepulveda, B., Otte, M.A., Rauf, S., Shiddiky, M.J., Trau, M., 2014. Chem. Commun. 50, 3585-3588.

Chang, H.W., Chow, V., Lam, K.Y., Wei, W.I., Yuen, A., 2002. Cancer. 94:386-92.

Das, J., Cederquist, K.B., Zaragoza, A.A., Lee, P.E., Sargent, E.H., Kelley, S.O., 2012. Nat. Chem. 4, 642-648.

Delpu, Y., Cordelier, P., Cho, W.C., Torrisani, J., 2013. Int. J. Mol. Sci. 14, 15029-15058.

Gowtham, S., Scheicher, R.H., Ahuja, R., Pandey, R., Karna, S.P., 2007. Phys. Rev. B. 76, article number 033401.

Herman, J.G., Graff, J.R., Myöhänen, S., Nelkin, B.D., Baylin, S.B. 1996. Proc. Natl. Acad. Sci. U. S. A. 93, 9821-9826.

Jones, P.A., Takai, D., 2001. Science. 293, 1068-1070.

Kasem, K., Gopalan, V., Salajegheh, A., Lu, C.T., Smith, R.A., Lam, A.K.Y., 2014. Exp Cell Res. 326, 166-173.

Kato, D., Goto, K., Fujii, S.-i., Takatsu, A., Hirono, S., Niwa, O., 2011. Anal. Chem. 83, 7595-7599.

Kato, D., Sekioka, N., Ueda, A., Kurita, R., Hirono, S., Suzuki, K., Niwa, O., 2008. J. Am. Chem. Soc. 130, 3716-3717.

Koo, K.M., Sina, A.A., Carrascosa, L.G., Shiddiky, M.J., Trau, M., 2014a. Analyst. 139, 6178-6184.

Koo, K.M., Wee, E.J., Rauf, S., Shiddiky, M.J., Trau, M., 2014b. Biosens. Bioelectron. 56, 278-285.

Kurita, R., Arai, K., Nakamoto, K., Kato, D., Niwa, O., 2012. Anal. Chem. 84, 1799-1803.

Kuroki, T., Trapasso, F., Yendamuri, S., Matsuyama, A., Alder, H., Mori, M., Croce, C.M., 2003. Clin. Cancer Res. 9, 1441-1445.

Long, C., Yin, B., Lu, Q., Zhou, X., Hu, J., Yang, Y., Yu, F., Yuan, Y., 2007. Cancer Invest. 25, 685-690.

Plongthongkum, N., Diep, D.H., Zhang, K., 2014. Nat. Rev. Genet. 15, 647-661.

Sina, A.A., Howell, S., Carrascosa, L.G., Rauf, S., Shiddiky, M.J., Trau, M., 2014. Chem. Commun. 50, 13153-13156.

Taleat, Z., Mathwig, K., Sudhölter, E.J.R., Rassaei, L., 2015. Trac- Trends Anal. Chem. 66, 80-89.

Tang, W.K., Chui, C.H., Fatima, S., Kok, S.H., Pak, K.C., Ou, T.M., Hui, K.S., Wong, M.M., Wong, J., Law, S., Tsao, S.W., Lam, K.Y., Beh, P.S., Srivastava, G., Chan, A.S., Ho, K.P., Tang, J.C., 2007. Int. J. Mol. Med. 19, 915-923.

Varghese, N., Mogera, U., Govindaraj, A., Das, A., Maiti, P.K., Sood, A.K., Rao, C.N.R., 2009. ChemPhysChem. 10, 206-210.

Wang, Y., Wee, E.J.H., Trau, M., 2016. Chem. Commun. 52, 3560-3563.

Wee, E.J., Rauf, S., Shiddiky, M.J., Dobrovic, A., Trau, M., 2015a. Clin. Chem. 61, 163-171.

Wee, E.J.H., Ha Ngo, T., Trau, M., 2015b. Sci. Rep. 5, article number15028.

Wojdacz, T.K., Dobrovic, A., 2007. Nucleic Acids Res. 35, e41.

Wong, M.L., Tao, Q., Fu, L., Wong, K.Y., Qiu, G.H., Law, F.B., Tin, P.C., Cheung, W.L., Lee, P.Y., Tang, J.C., Tsao, G.S., Lam, K.Y., Law, S., Wong, J., Srivastava, G., 2006. Int. J. Oncol. 28, 767-773.

Wong, T.S., Man, M.W., Lam, A.K., Wei, W.I., Kwong, Y.L., Yuen, A.P., 2003. Eur. J. Cancer. 39, 1881-1887.

Wu, M., Kempaiah, R., Huang, P.-J.J., Maheshwari, V., Liu, J., 2011. Langmuir. 27, 2731-2738.

Wu, S.C., Zhang, Y., 2010. Nat. Rev. Mol. Cell. Biol. 11, 607-620.

Zhang, J., Wang, L., Pan, D., Song, S., Fan, C., 2007. DNA hybridization "turns on" electrocatalysis at gold electrodes. Chem. Commun. 11, 1154-1156.

Zhang, J.J., Zhang, L., Zhou, K., Ye, X., Liu, C., Zhang, L., Kang, J., Cai, C. 2011. Anal Biochem. 413,164-170.

Zhang, L., Xu, Y.-Z., Xiao, X.-F., Chen, J., Zhou, X.-Q., Zhu, W.-Y., Dai, Z., Zou, X.-Y., 2015. Trac- Trends Anal. Chem. 72, 114-122.

Figure Captions

Fig. 1. Schematic of graphene-DNA adsorption based methylation assay. The adsorption of ss-DNA on g-SPCE repulse $[Fe(CN)_6]^{3-}$ molecules from accessing electrode surface, providing a significate DPV signal. Inset, typical differential pulse voltammetric signals showing the guanine-enriched methylated DNA that produces lower DPV currents in comparison to the adenine-enriched unmethylated DNA.

Fig. 2. Left, Differential pulse voltammetric current changes with respect to the designated CpG sites. Right, typical DPV signal for the sample containing 1 CpG site and its corresponding background signal. Each data point represents the average of three repeat trails, and error bars represent the standard deviation of measurements (%RSD = <5% for n = 3).

Fig. 3. Differential pulse voltammetric current changes with respect to the designated methylation level. Inset, typical DPV signals for the sample containing 5% (left, top) and 95% (right, bottom) and their corresponding background signals. Each data point represents the average of three repeat trails, and error bars represent the standard deviation of measurements (%RSD = <5% for n = 3).

Fig. 4. Relative current changes for detecting *FAM134B* promoter region in (**A**) three oesophageal cancer cell lines and unmethylated, and (**B**) two normal (N1 and N2) and six (P1-P6) oesophageal cancer tissue samples. Each data point represents the average of three

repeat trails, and error bars represent the standard deviation of measurements (%RSD = <5% for n = 3).

Figures

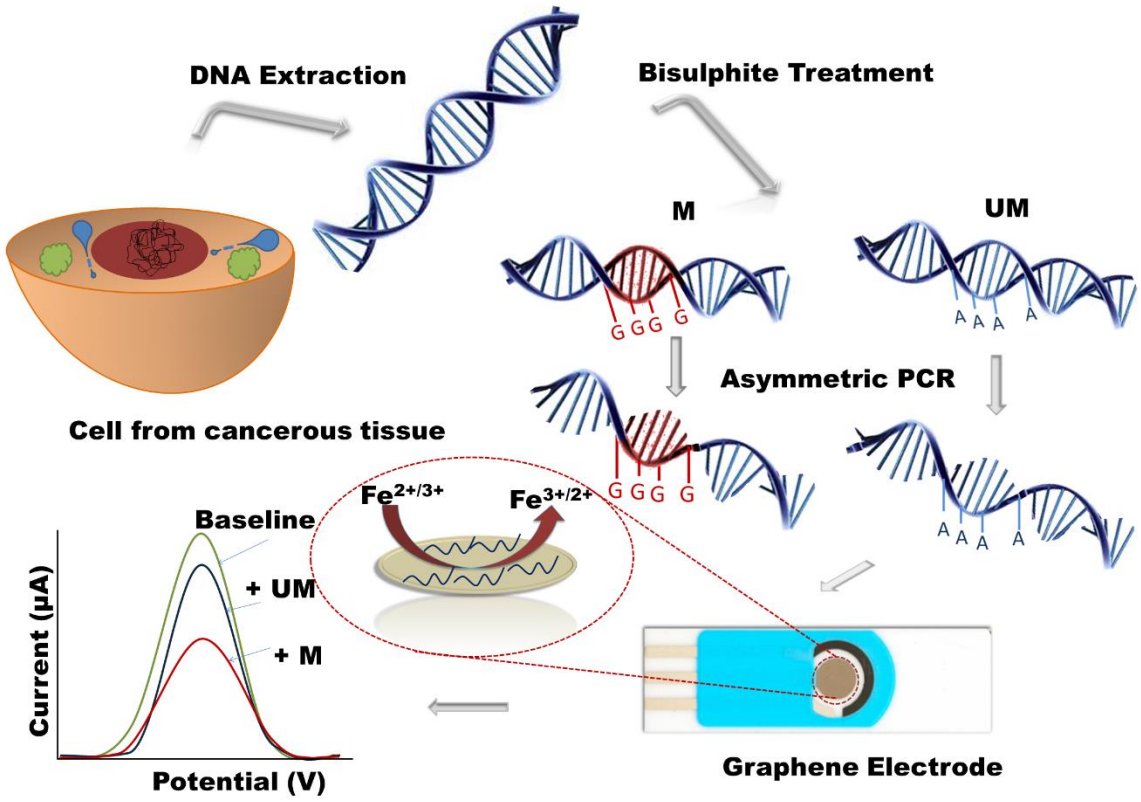

Fig. 1

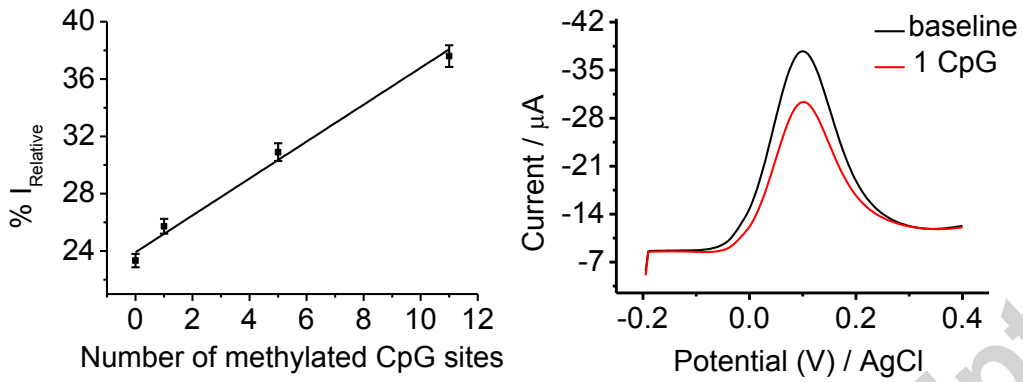

Fig. 2

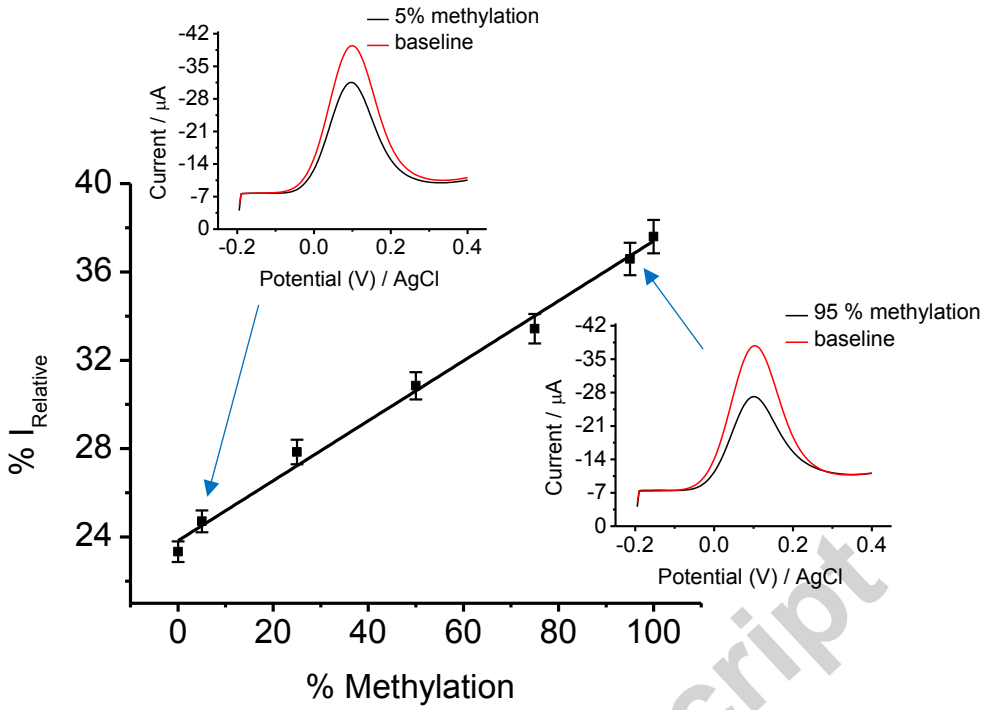

Fig. 3

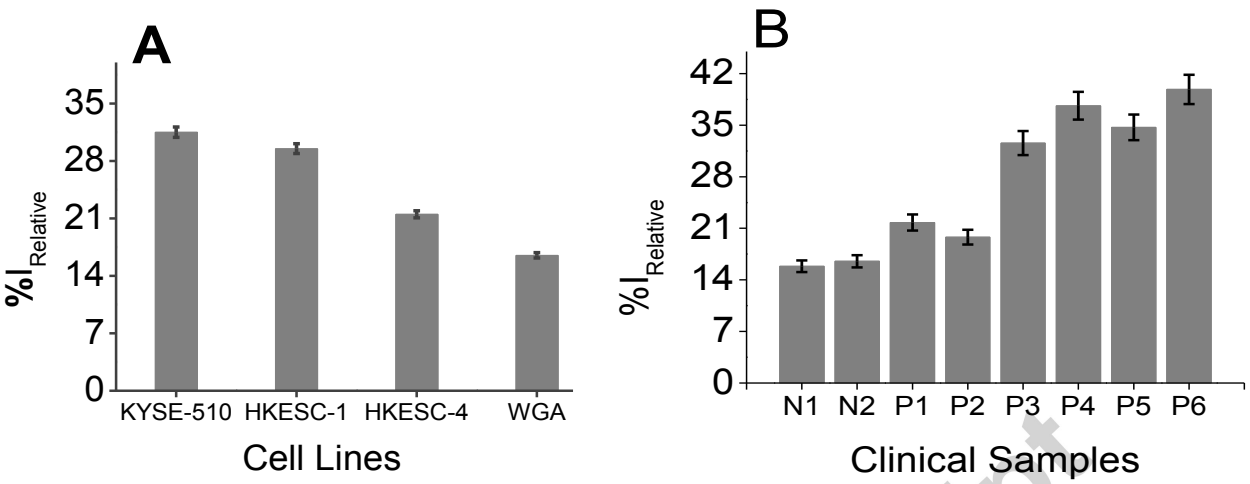

Fig. 4